Chinese Chemical Letters 36 (2025) 109884

Contents lists available at ScienceDirect

Chinese Chemical Letters

journal homepage: www.elsevier.com/locate/cclet

Non-specific/specific SERS spectra concatenation for precise bacteria classifications with few samples using a residual neural network

Feihu Wu[a,1], Gengwen Chen[b,1], Kaitao Lai[a], Shiqing Zhang[a], Yingchao Liu[a], Ruijian Luo[a], Xiaocong Wang[a], Pinzhi Cao[a], Yi Ye[b], Jiarong Lian[a], Junle Qu[a], Zhigang Yang[a,*], Xiaojun Peng[c]

[a] Shenzhen Key Laboratory of Photonics and Biophotonics & College of Physics and Optoelectronic Engineering, Key Laboratory of Optoelectronic Devices and Systems of Ministry of Education and Guangdong Province, Shenzhen University, Shenzhen 518060, China
[b] Hematology Reagent R&D department, Mindray Bio-medical Electronics Co., LTD., Shenzhen 518107, China
[c] State Key Laboratory of Fine Chemicals, College of Material Science and Engineering, Shenzhen University, Shenzhen 518060, China

ARTICLE INFO

Article history:
Received 22 December 2023
Revised 26 March 2024
Accepted 10 April 2024
Available online 11 April 2024

Keywords:
SERS
Deep learning
Resnet
Bacteria classification
Spectra concatenation

ABSTRACT

Deep learning neural network incorporating surface enhancement Raman scattering technique (SERS) is becoming as a powerful tool for the precise classifications and diagnosis of bacterial infections. However, the large amount of sample requirement and time-consuming sample collection severely hinder its applications. We herein propose a spectral concatenation strategy for residual neural network using non-specific and specific SERS spectra for the training data augmentation, which is accessible to acquiring larger training dataset with same number of SERS spectra or same size of training dataset with fewer SERS spectra, compared with pure non-specific SERS spectra. With this strategy, the training loss exhibit rapid convergence, and an average accuracy up to 100% in bacteria classifications was achieved with 50 SERS spectra for each kind of bacterium; even reduced to 20 SERS spectra per kind of bacterium, classification accuracy is still >95%, demonstrating marked advantage over the results without spectra concatenation. This method can markedly improve the classification accuracy under fewer samples and reduce the data collection workload, and can evidently enhance the performance when used in different machine learning models with high generalization ability. Therefore, this strategy is beneficial for rapid and accurate bacteria classifications with residual neural network.

Bacterial infections have become a major concern for the global health. Different bacteria lead to diverse symptoms such as mild gastrointestinal inflammation, wound infections and severely lethal diseases, badly threating to human health [1,2]. With the increasing bacterial infection, new challenges have emerged in the treatments. It leads to overuse of antibiotics, which further affects the success and cost of treatment [3]. The clinical gold standard of blood culturing method exhibits high accuracy in bacterial inspection but low efficiency and time-consuming [4,5]. The patient have to accept broad-spectrum antibiotics treatment prior to the diagnosis results [6], which is actually unnecessary for every patient. Therefore, rapid, accurate and sensitive diagnosis have become extremely urgent in public health and medical areas.

Deep learning neural network based artificial intelligent have recently become a powerful analytic tool incorporating with sensitive detect techniques, such as multiparametric MRI for cancer diagnosis [7–12]. Surface-enhanced Raman Scattering (SERS) technique [13–17] is capable of detection of low abundance of targets with rapid response and high sensitivity, which exhibits excellent performance in tiny difference identifications between clinical specimens from the fingerprint information [18–21]. And deep learning algorithms using for SERS spectra have showed promising capability in bacteria and cancer classifications with high precision [22,23]. However, deep learning neural networks usually require for large training datasets to facilitate for accurate diagnosis [24], but generally spend long time for the sample collections and consume a lot of workloads to carry out the SERS spectral measurements. Therefore, it is necessary to develop new method for deep learning with small training dataset without reduction of the classification accuracy.

* Corresponding author.
E-mail address: zhgyang@szu.edu.cn (Z. Yang).
[1] These authors contributed equally to this work.

https://doi.org/10.1016/j.cclet.2024.109884
1001-8417/

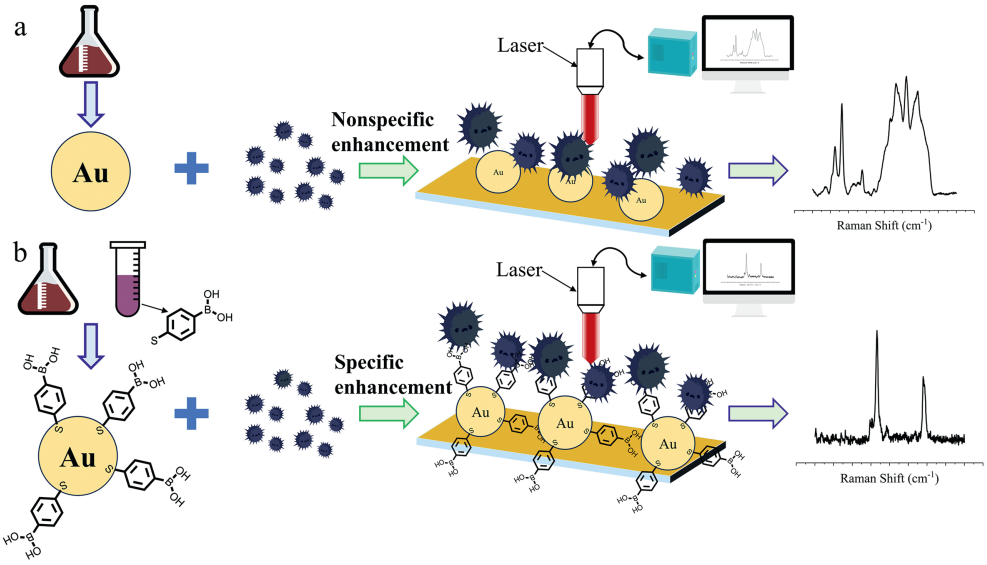

Scheme 1. Schematic diagram of non-specific/specific SERS spectral acquisition. (a) Procedure for AuNPs preparation and non-specific SERS spectra acquired by interaction of AuNPs and bacterial samples. (b) The functionalization of AuNPs by 4-mercaptophenylboronic acid and specific SERS spectra acquired by covalent interaction of phenylboronic acid with the diol groups in the surface of bacteria.

To address above issues, we herein propose a new strategy of SERS spectral concatenation for residual neural network to achieve rapid and precise bacteria classification with few samples, of which the training dataset with enhanced information abundance can be acquired by data concatenation from randomly selection of non-specific and specific SERS spectra. In this work, we first measured non-specific/specific SERS spectra from the interaction of gold nanoparticles (40 nm AuNPs)/4-mercaptophenylboronic acid fabricating gold nanoparticles (80 nm AuNPs@4MPBA) and bacteria samples (11 species), respectively. Non-specific SERS spectra provide universal features and background information, while specific SERS spectra offer unique feature of a peptidoglycan on the bacterial surface, enabling specific enhancement through the change of Raman intensities at feature peaks (Scheme 1) [25–27]. By combining both SERS spectra, the resulting dataset contains more comprehensive representation of the sample with diverse information. With increasing information content of training, validating and testing dataset, the residual deep learning algorithms can extract more feature information for precise spectral analysis, which help to perform high precision of bacterial classifications with fewer samples and robust analysis of disparate data [28]. In addition, the method can accelerate the training convergence, beneficial for fast training and accurate diagnosis.

Bacterial suspension (1 mL) was removed from the blood culture bottles and centrifuged at 1200 rpm/min for 5 min, the supernatant was discarded and the sediment was dispersed in 500 μL of sterile water. The solution should be freshly prepared before the experimental test. The obtained AuNPs solution (10 μL) was mixed with the bacterial solution (10 μL), and suspended at room temperature for 30 min. And the 4-MPBA@AuNPs solution (10 μL) was added into the bacterial solutions (10 μL) to place into a water bath at 37 °C for a while, which make sure the occurrence of the reaction between AuNPs@4-MPBA and bacteria. The 4-mercaptophenylboronic acid is readily to covalently bind with vicinal diol groups of the saccharide on the surface of the bacteria. The mixture of AuNPs and bacteria obtained was pipetted a small amount of solution drops onto the gold-plated sheet to dry it naturally. The SERS spectra were acquired using a 785 Raman spectrometer with the laser power set to 33 mW and the integration time to 5 s. Non-specific spectral acquisition was performed on the dried samples, and 10 positions were randomly selected to take the non-specific SERS spectra for each sample, which help to acquire the complete features. In contrast, the reaction mixture of 4MPBA@AuNPs and bacteria was subsequently measured to provide specific SERS spectra. In total, 550 non-specific spectra and 550 specific spectra from 11 bacterial species were collected as the experimental method, and the bacteria samples were provided by Mindray Bio-medical Electronics Co., LTD. The species of the bacteria samples can be seen in Table S1 (Supporting information).

Gold nanoparticles (AuNPs, 40 and 80 nm in size) were first prepared by the reduction of chloroauric acid with different amounts of trisodium citrate in the boiling water (Supporting information). And the obtained AuNPs was uniformly dispersed in water with an ellipsoidal shape characterized by a TEM (Fig. 1a and Fig. S1 in Supporting information) and UV absorption spectra (Fig. S3 in Supporting information). Then, 4-mercaptopyridine (4-MPy) was utilized to test the sensitivity of AuNPs to be *ca.* 0.9 μmol/L (Fig. 1b), indicating the quantified enhancement of AuNPs. In addition, 80 nm-sized AuNPs were further fabricated with 4-mercaptophenylboronic acid (AuNPs@4MPBA), which was verified by SERS spectral variations and FTIR spectra (Fig. S2 in Supporting information). It can be seen typical feature peaks for the phenyl, C-S, C-B bonds at the range of 500–1600 cm^{-1} and there is a vibrational peak of BO–H at 3420 cm^{-1} in Fig. S2b (Supporting information), which means that 4MPBA successfully anchored to the surface of AuNPs. And for the gold nanoparticles without modifications, it can be also observed some small peaks in the same region, ascribed to the binding of ascorbate in the preparation of the gold nanoparticles. Two featuring peaks of phenylboronic acid were found at 1060 and 1560 cm^{-1} with the signal enhancement of Rhodamine 6 G, which indicates the 4-MPBA successfully anchored to the surface of the AuNPs (Fig. 1c). Moreover, the Raman intensity at 1060 cm^{-1} and 1560 cm^{-1} was increased with the titration of glucose, which show high sensitivity and selectivity of AuNPs@4-MPBA to sugars (Fig. 1d). All the results demonstrate that both AuNPs (40 nm) and AuNPs@4-MPBA (80 nm) can be employed for the non-specific and specific SERS measurement of bacteria specimen, respectively.

The non-specific and specific SERS spectra were acquired from 11 kind of bacteria to make up the training dataset, which were measured upon the interaction of bacteria samples with AuNPs (40 nm) and AuNPs@4-MPBA (80 nm), respectively. Each bacte-

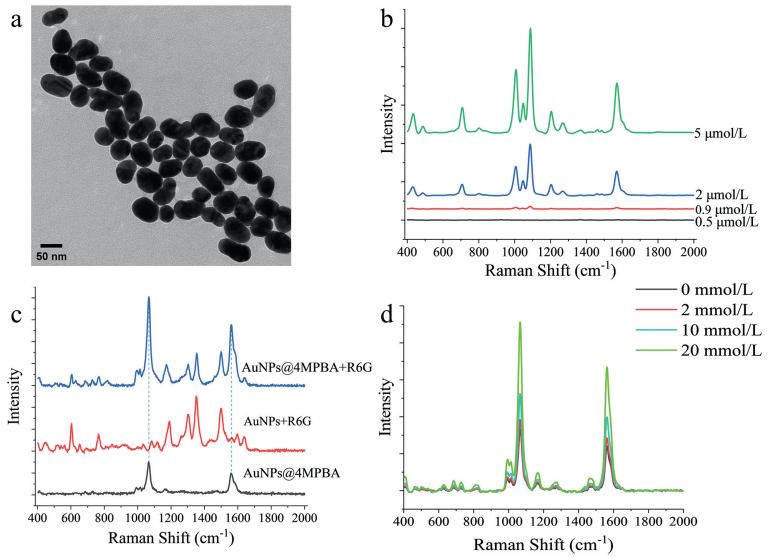

Fig. 1. The characterization of AuNPs and AuNPs@4MPBA using TEM and SERS spectra. (a) TEM image of AuNPs showing ellipsoidal morphology. (b) Detect sensitivity of AuNPs to 4-MPy, laser power: 33 mW and the integration time: 5 s. (c) SERS test of AuNPs@4-MPBA on Rhodamine 6G (R6G), with characteristic peaks appearing at 1067 and 1560 cm^{-1}, and also exhibiting a non-specific enhancement effect. (d) SERS spectral titrations of AuNPs@4-MPBA with glucose with feature peak changes at 1067 and 1560 cm^{-1}.

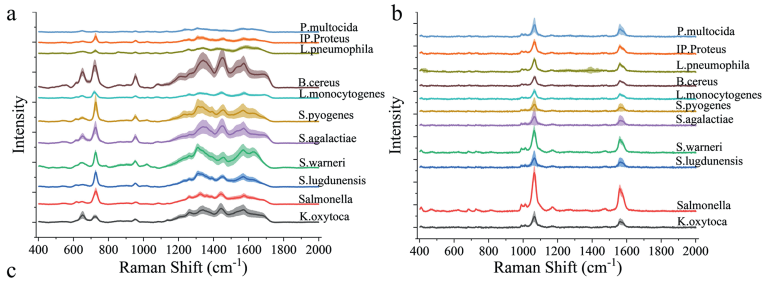

c

Raman Shift (cm^{-1})	Functional groups or Substances
645-660	C-S stretching & C-C twisting of tyrosine, proteins *etc.*
716-735	DNA
948-964	Amino acids proline and valine and polysaccharides lipid
1319-1345	CH_3CH_2 wagging mode in collagen & purine of DNA
1435-1450	CH_2 deformation (Lipid, *etc.*)

Fig. 2. SERS spectra of different bacteria interaction with AuNPs and AuNPs@4MPBA, respectively; and peak identifications of the SERS spectra. (a) The non-specific SERS spectra of AuNPs interaction with 11 bacteria. (b) The specific SERS spectra of AuNPs@4MPBA interaction with 11 bacteria. (c) Non-specific SERS spectral identification of AuNPs interaction with 11 bacteria. *Klebsiella oxytoca* (*K. oxytoca*), *Salmonella*, *Staphylococcus lugdunensis* (*S. lugdunensis*), *Staphylococcus warneri* (*S. warneri*), *Streptococcus agalactiae* (*S. agalactiae*), *Staphylococcus pyogenes* (*S. pyogenes*), *Listeria monocytogenes* (L. *monocytogenes*), *Bacillus cereus* (*B. cereus*), *Legionella pneumophila* (*L. pneumophila*), *Indole-Positive Proteus* (*IP. Proteus*), *Pasteurella multocida* (*P. multocida*).

ria sample was measured for 10 spectra every time (five times in total finished in 5 days). In the experiment, the mixture of AuNPs and AuNPs@4-MPBA with bacteria solution were dripped onto slides coated with 200 nm-thick gold film and dry naturally (Fig. S4 in Supporting information) and were measured under the excitation laser power of 33 mW with the integration time of 5 s. Each bacterium was continuously tested for 5 days to offer a comprehensive data. From the non-specific SERS spectra (Fig. 2a), tiny difference can be observed at all peaks, which is difficult to distinguish through traditional methods. Meanwhile, the specific SERS spectra were collected under the same experimental conditions using AuNPs@4-MPBA (Fig. 2b). From both SERS spectra, it can be found that the SERS spectra from the same bacteria show slight changes in different measurements. And the peaks at the SERS spectra are identified to the biological targets, such as proteins, DNA, amino acids (Fig. 2c). The spectra show differentiable changes at the featured peaks with the interaction of bacterial peptidoglycan. Different SERS intensity can be obtained when adding different bacteria species into the nanoparticle solution. However, the specific SERS intensity is not enough to represent all features for bacteria identifications. Therefore, the combination of both specific and non-specific SERS spectra can increase information abundance for precise classification when used for deep learning algorithms (Fig. S7 in Supporting information).

To perform the deep learning analysis of SERS spectra, a residual deep learning neural network was constructed with data-pretreatment layer, six residual blocks, CNN (1D) layers, batch normalization (1D) layers, fully connected layers and a Softmax function output layer [23]. Prior to the feature extraction through convolutional layers, the specific and non-specific SERS data were pretreated for background perturbation subtraction and baseline corrections using the airPLS algorithm and data concatenations (along with dim = 1) of randomly selected non-specific and specific SERS spectrum, respectively. This procedure can increase the data quality with more information content. And then the obtained concate-

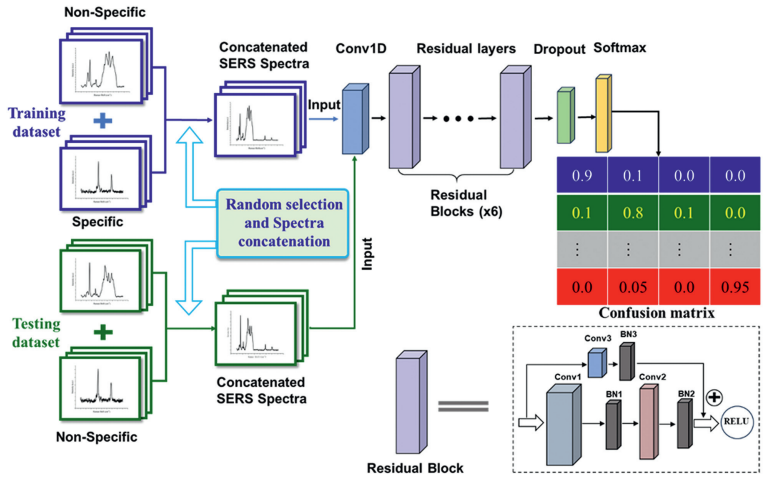

Fig. 3. Schematic diagram of the residual neural network. A residual block consisting of 1 initial convolutional layer, 6 residual modules and a dropout layer.

nated spectral data were prepared for training, validating and testing dataset. The training dataset was input into the convolutional layers to extract the local features, which helps to capture the exact information such as peaks and troughs in the spectrum to enhance the classification ability. The residual layer allows information from the previous layer directly passing to the subsequent layers through jump connections, thus maintaining a steady transfer of important features. And six residual layers were introduced into the present network to acquire deep features to mitigate the gradient vanish during back propagation, which can train the network model more efficiently to avoid the overfitting. And a dropout layer was incorporated into the neural network to enhance the generalization ability by randomly dropping some neurons, which help to prevent the model from overdependence on specific data and to exclude overfitting. Last, the extracted high-level features are mapped to the final category label space using the fully connected layer, and the probability is normalized by the Softmax function to show the predicted probability of each category (Fig. 3).

To approve the feasibility of SERS spectral concatenation strategy utilized in the residual deep learning model, the dataset with different compositions were introduced into the neural network for the performance comparison. Initially, 11 kinds of bacteria were selected to do the non-specific and specific SERS measurements with signal enhanced by AuNPs and AuNPs@4-MPBA, respectively. Each bacterial sample was taken for 10 specific and 10 non-specific SERS spectra every time and was measured successively for 5 times (one time per day, 5 days in total), which 100 SERS spectra can be obtained for each bacterium and 1100 spectra were accessible in total. Then the obtained dataset (6875 spectra at most) was splicing by 50 SERS spectra randomly selected from the experimental data (50 pure non-specific SERS spectra, or 25 non-specific and 25 specific SERS spectra from each of the 11 bacterial species, respectively). And the concatenated dataset was randomly shuffled and equally divided into two parts: One part was further split into the training and validation dataset as the assigned ratio; and the other was used as the testing dataset for model training and evaluation. From training/validation loss curve in Fig. 4a, the dataset composed of 25 non-specific and 25 specific spectra shows the fastest convergence to reach the optimal performance metrics at the 7^{th} epoch with the final validation accuracy higher up to 100% (Fig. 4b). In contrast, the data was obtained from 50 pure specific or non-specific SERS spectra, for 30 training epochs, the model cannot reach convergence until 20^{th} epoch (green plot in Fig. 4c) with a validation accuracy of 93.5% (orange curve in Fig. 4d). And different SERS spectral concatenations was further performed to prove good performance and significant improvements to bacterial classification (Fig. 4e). Additionally, the present method was also performed with small dataset of 10 spectra concatenated by 5 non-specific and 5 specific SERS spectra, independently, of which the training loss showed slower convergence and the test accuracy is still up to 97.8%, much higher than that of 10 pure non-specific SERS spectra (Figs. S10-S17 in Supporting information). Therefore, the proposed strategy presents better performance in the classification accuracy using smaller sample size, which enable the reduction of training dataset for deep learning model. This will help to save the workload of data acquirement and to shorten the time for sample collection.

The superiority of the residual deep learning model trained under present condition was further exploited on extra samples. From the 11 bacteria species, 10 SERS spectra for each bacterium were measured every day in the period of 5 days to make up the dataset. And 40 non-specific SERS spectra for each bacterium measured in 4 days were randomly selected for the training dataset, and 10 SERS spectra left measured in the 5^{th} day were used for the extra test dataset. And then, 20 non-specific spectra and 20 specific spectra from each bacterium acquired in the 4 days were randomly selected to concatenate alongside dim = 1 for the training dataset, and 10 non-specific and 10 specific SERS spectra for each bacterium obtained in the 5^{th} day were concatenated for the test dataset. The two group of datasets were input into the neural network for the training procedure upon data pretreatment; it can be seen from the confusion matrix in Figs. 5a and b, the training accuracy using only 40 non-specific spectra is 83.6%, and the combination of 20 non-specific and 20 specific SERS spectra is 96.3%, which exhibit higher accuracy and faster convergence in training stage, even in the case of few samples. Furthermore, we also calculated the t-distributed stochastic neighbor embedding (t-SNE) plots with the training results from the two methods, which are commonly used in biological classifications. If the stronger the correlation between two categories, the closer they are presented on the plots; on the contrary, the two categories are far away from each other. As shown in Figs. 5c and d, it can be poorly classified using only non-specific spectra, of which some category points are still overlapping to each other. In contrast, the precise classifications using the spectra concatenation was achieved with each category separated far away from each other and the same categories clustered together. And the detection sensitivity of the latter is also higher than that of the former (Fig. 5e).

We further compressed the training dataset by splicing 10 non-specific and 4 specific SERS spectra extracted from the 40 spectra,

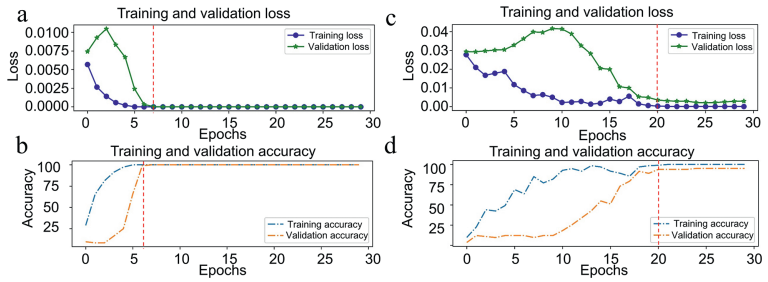

e

	Sample number	Epochs	Training accuracy	Validation accuracy	Test accuracy	Convergence speed
AuNPs	50	30	1.000	0.935	0.956	20
AuNPs	25	30	1.000	0.893	0.884	20
AuNPs	10	30	0.988	0.783	0.782	30
4MPBA@AuNPs + AuNPs	25×25	30	1.000	1.000	1.000	7
4MPBA@AuNPs + AuNPs	10×10	30	1.000	1.000	0.996	20
4MPBA@AuNPs + AuNPs	10×5	30	1.000	1.000	0.993	17
4MPBA@AuNPs + AuNPs	5×5	30	1.000	1.000	0.957	17

Fig. 4. Training and validation plots of loss and accuracy with different spectral concatenation ratios. (a) Training loss curves of 30 epoch training using 25 non-specific spectra and 25 specific spectra concatenated alongside dim = 1 to produce a total of 6875 spectra ($25 \times 25 \times 11$). (b) Training accuracy curves of 30 epoch training using 25 non-specific spectra and 25 specific spectral concatenation. (c) Training loss curves of 30 epoch training using 550 non-specific spectra. (d) Training accuracy curves of 30 epoch training using 550 non-specific spectra. (e) The performance metrics for different concatenations.

Table 1
Individual model network metrics.

NPs	AuNPs					AuNPs@4MPBA+AuNPs				
Model	Precision	Recall	Specificity	Train accuracy	Test accuracy	Precision	Recall	Specificity	Train accuracy	Test accuracy
Resnet	0.918	0.904	0.988	1.00	0.884	0.996	0.996	0.999	1.000	0.996
VGG-16	0.716	0.712	0.969	0.822	0.688	0.823	0.864	0.986	0.883	0.862
SVM	0.937	0.948	0.994	1.000	0.935	1.000	1.000	1.000	1.000	1.000
Dec-Tree	0.738	0.744	0.971	1.000	0.710	0.993	0.993	0.999	1.000	0.999
KNN	0.750	0.746	0.971	0.898	0.703	0.982	0.987	0.998	0.998	0.980

both the new dataset contained 40 combined SERS spectra at the same size with the pure 40 non-specific SERS, and remaining the same size of test set (Fig. S9 in Supporting information). The final classification accuracy was calculated to be 93.6%. The reduction of the training set did not deteriorate the overall performance of the model, all of which the concatenation of non-specific and specific SERS spectra increases the information abundance and the feature number to ensure the high classification accuracy. Last, to test the adaptability of the model on unknown samples, we collected the SERS spectra of new bacteria of the same species, each of which was collected 20 non-specific spectra and non-specific spectra and was divided to make training and test dataset and concatenated into 1100 spectra. The new training dataset was mixed with the previous training dataset, while the test dataset was operated in the same way and the model was retrained and tested with a classification accuracy up to 98% as seen in the confusion matrix (Fig. S18 in Supporting information), demonstrating that the model trained by this method can be well applied to new datasets with good adaptability.

To further explore the broad applicability of the present method in different algorithms, we selected 25 non-specific SERS spectra, as well as a dataset acquired from the concatenation of 10 specific and 10 non-specific SERS spectra to test different algorithms, including ResNet, VGG-16, and traditional machine learning models such as support vector machine (SVM), Decision-Tree, and K-Nearest Neighbor (KNN). The experimental results clearly revealed that the spectral concatenation method show marked improvement in the training/test accuracies as well as the corresponding metrics (precision, recall and specificity), which proved the excellent generalization ability of the proposed strategy in both deep learning models and traditional machine learning models (Table 1).

In conclusion, a new strategy of non-specific and specific SERS spectral concatenation was developed to pretreat the training data fit for deep learning neural network. Upon background subtraction and baseline correction using airPLS algorithm, the SERS spectra were selected to splice along with assigned dimension to increase information abundance, which showed faster convergence and better performance metrics than pure non-specific SERS data when input into the residual neural network. Compared with non-specific SERS spectra (50 spectra), the same amount of 25 non-specific-25 specific SERS spectra (50 spectra) can provide larger amount of concatenated spectra (625 spectra) with large increase of feature information content; And the same size of concatenated spectra (50 spectra) can be obtained by the combination of 10 non-specific and 5 specific SERS spectra (15 spectra), which achieve to offer large amount of training data with fewer sample or markedly save workload and time for sample collection. With this strategy, we achieved to perform the bacteria classification with high accuracies (100% in model training, 96.3% in extra test of large sample size and 93.6% in extra test of small sample) and faster convergence in training process, proved the feasibility of the strategy with smaller sample size. Not only that, the model trained using this method can also be well applied to the new dataset, and the new model can be retrained with only a slight modification of the dataset. Moreover, it can be generally incorporate with diverse machine learning algorithms with marked increase of performance metrics, which improve the performance of traditional deep learning models incapable of precise and rapid analysis without enough samples.

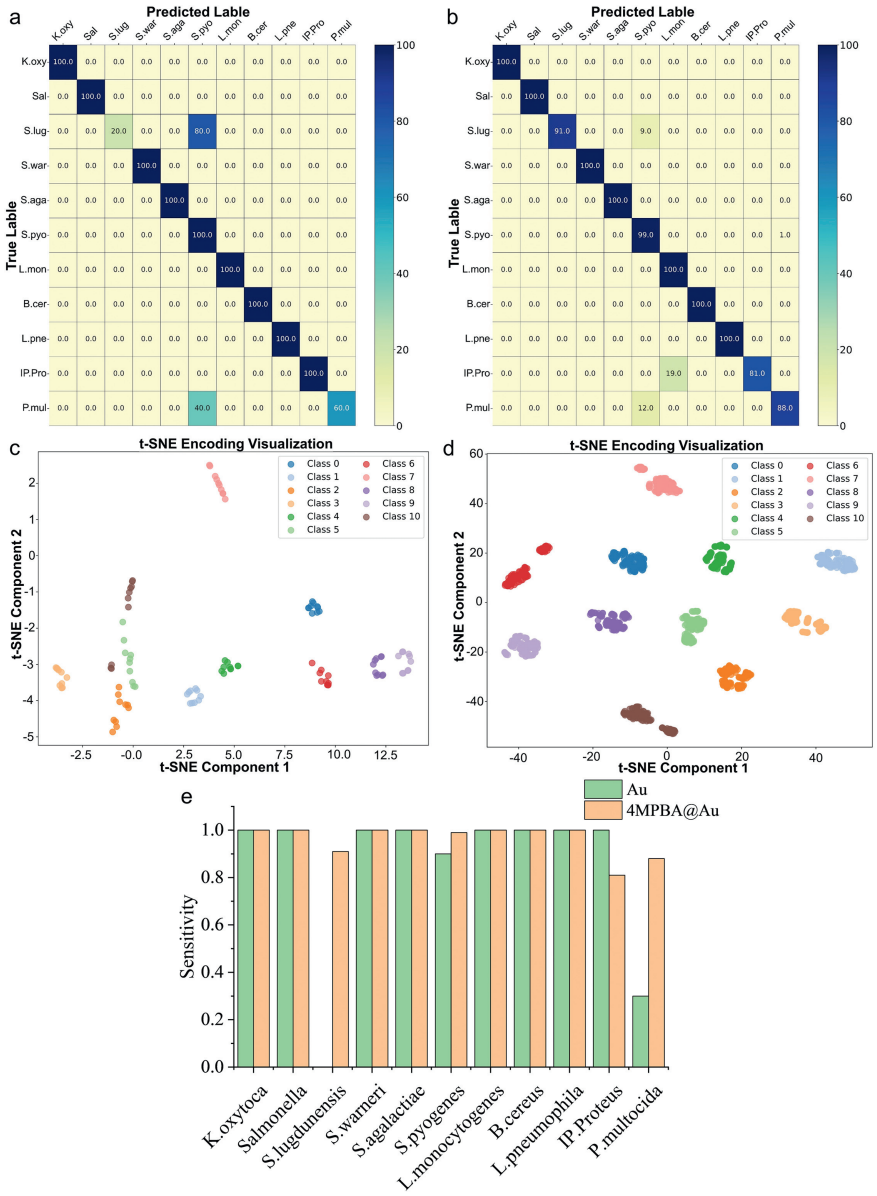

Fig. 5. Confusion matrix for the non-specific SERS spectra alone and non-specific/specific SERS spectral concatenation and dataset processing. (a) Testing of extra unknown samples using the trained model with non-specific spectra. (b) Testing of extra un-known samples using a trained model with the spectral concatenation of non-specific and specific spectra. (c) t-SNE plot for test classification using models trained with non-specific spectra. (d) t-SNE plot for test classification using models trained with the spectral concatenation of non-specific and specific spectra. (e) The sensitivity obtained by the methods.

Declaration of competing interest

The authors declare that they have no known competing financial interests or personal relationships that could have appeared to influence the work reported in this paper.

CRediT authorship contribution statement

Feihu Wu: Data curation, Formal analysis, Writing – original draft. **Gengwen Chen:** Data curation, Investigation, Resources. **Kaitao Lai:** Methodology. **Shiqing Zhang:** Validation. **Yingchao Liu:** Validation. **Ruijian Luo:** Investigation. **Xiaocong Wang:** Visualization. **Pinzhi Cao:** Investigation. **Yi Ye:** Resources, Validation. **Jiarong Lian:** Funding acquisition, Writing – review & editing. **Junle Qu:** Writing – review & editing. **Zhigang Yang:** Writing – original draft, Writing – review & editing, Conceptualization, Funding acquisition, Methodology, Project administration, Supervision. **Xiaojun Peng:** Writing – review & editing.

Acknowledgments

This work was partially supported by the National Key Research and Development Program of China (No. 2023YFC3402900), the National Nature Science of Foundation (No. 61875131); Shenzhen Key Laboratory of Photonics and Biophotonics (No. ZDSYS20210623092006020); Shenzhen Science and Technology Innovation Program (No. 20231120175730001); and Prof. Zhigang Yang wants to thank Prof. Zhenhua Sun from college of physics and optoelectronic engineering, Shenzhen University for his kind help in the preparation of reflective mirror covered with gold film (200 nm).

Supplementary materials

Supplementary material associated with this article can be found, in the online version, at doi:10.1016/j.cclet.2024.109884.

References

[1] C. Fleischmann, A. Scherag, N.K.J. Adhikari, et al., Am. J. Respir. Crit. Care Med. 193 (2016) 259–272.
[2] R. DeAntonio, J.P. Yarzabal, J.P. Cruz, J.E. Schmidt, J. Kleijnen, Hum. Vaccines Immunother. 12 (2016) 2422–2440.
[3] X. Pang, Q. Xiao, Y. Cheng, et al., ACS Nano 13 (2019) 2427–2438.
[4] R.P. Dellinger, M.M. Levy, A. Rhodes, et al., Intensive Care Med. 39 (2013) 165–228.
[5] A. Chaudhuri, P.M. Martin, P.G.E. Kennedy, et al., Eur. J. Neurol. 15 (2008) 649–659.
[6] Am. J. Respir. Crit. Care Med. 171 (2005) 388–416, doi:10.1164/rccm.200405-644ST.
[7] X.X. Chen, X.M. Wang, K. Zhang, et al., Med. Image Anal. 79 (2022) 102444.
[8] H. Shin, S. Oh, S. Hong, et al., ACS Nano 14 (2020) 5435–5444.
[9] F. Lussier, V. Thibault, B. Charron, G.Q. Wallace, J.F. Masson, TrAC Trends Anal. Chem. 124 (2020) 115796.
[10] B.E. Bejnordi, M. Veta, P.J. van Diest, et al., J. Am. Med. Assoc. 318 (2017) 2199–2210.
[11] V. Gulshan, L. Peng, M. Coram, et al., J. Am. Med. Assoc. 316 (2016) 2402–2410.
[12] Q. Hu, H.M. Whitney, M.L. Giger, Sci. Rep. 10 (2020) 10536.
[13] X.X. Han, R.S. Rodriguez, C.L. Haynes, Y. Ozaki, B. Zhao, Nat. Rev. Methods Primers 1 (2021) 87.
[14] X.T. Wang, L. Guo, Angew. Chem. Int. Ed. 59 (2020) 4231–4239.
[15] D. Li, D.M. Yao, C.N. Li, et al., TrAC Trends Anal. Chem. 127 (2020) 115885.
[16] H.K. Lee, Y.H. Lee, C.S.L. Koh, et al., Chem. Soc. Rev. 48 (2019) 731–756.
[17] L.A. Lane, X. Qian, S. Nie, Chem. Rev. 115 (2015) 10489–10529.
[18] X. Zhou, Z.W. Hu, D.T. Yang, et al., Adv. Sci. 7 (2020) 2001739.
[19] S.E.J. Bell, G. Charron, E. Cortés, et al., Angew. Chem. Int. Ed. 59 (2020) 5454–5462.
[20] C. Zong, M.X. Xu, L.J. Xu, et al., Chem. Rev. 118 (2018) 4946–4980.
[21] H.Y. Wang, Y.F. Zhou, X.X. Jiang, et al., Angew. Chem. Int. Ed. 54 (2015) 5132–5136.
[22] H. Shin, B.H. Choi, O. Shim, et al., Nat. Commun. 14 (2023) 1644.
[23] C.S. Ho, N. Jean, C.A. Hogan, et al., Nat. Commun. 10 (2019) 4927.
[24] R.K. Samala, H.P. Chan, L.M. Hadjiiski, et al., Phys. Med. Biol. 62 (2017) 8894.
[25] L.B. Zheng, P. Qi, D. Zhang, Sens. Actuator B: Chem. 260 (2018) 983–989.
[26] P.X. Wang, S. Pang, B. Pearson, et al., Anal. Bioanal. Chem. 409 (2017) 2229–2238.
[27] S. Sankoh, C. Thammakhet, A. Numnuam, et al., Biosens. Bioelectron. 85 (2016) 743–750.
[28] F.A. Spanhol, L.S. Oliveira, P.R. Cavalin, C. Petitjean, L. Heutte, Deep features for breast cancer histopathological image classification, in: 2017 IEEE International Conference on Systems, Man, and Cybernetics, 2017, pp. 1868–1873.